Cell Metabolism
Article

Canonical Nlrp3 Inflammasome Links Systemic Low-Grade Inflammation to Functional Decline in Aging

Yun-Hee Youm,[1] Ryan W. Grant,[1] Laura R. McCabe,[2] Diana C. Albarado,[1] Kim Yen Nguyen,[1] Anthony Ravussin,[1] Paul Pistell,[1] Susan Newman,[1] Renee Carter,[3] Amanda Laque,[1] Heike Münzberg,[1] Clifford J. Rosen,[4] Donald K. Ingram,[1] J. Michael Salbaum,[1] and Vishwa Deep Dixit[1,5,*]

[1]Pennington Biomedical Research Center, LSU System, Baton Rouge, LA 70808, USA
[2]Department of Physiology, Michigan State University, East Lansing, MI 48824, USA
[3]Department of Veterinary Clinical Sciences, School of Veterinary Medicine, LSU, Baton Rouge, LA 70803, USA
[4]Center for Clinical and Translational Research, Maine Medical Center Research Institute, Scarborough, ME 04074, USA
[5]Section of Comparative Medicine and Department of Immunobiology, Yale University School of Medicine, New Haven, CT 06520,USA
*Correspondence: vishwa.dixit@yale.edu
http://dx.doi.org/10.1016/j.cmet.2013.09.010

SUMMARY

Despite a wealth of clinical data showing an association between inflammation and degenerative disorders in the elderly, the immune sensors that causally link systemic inflammation to aging remain unclear. Here we detail a mechanism by which the Nlrp3 inflammasome controls systemic low-grade age-related "sterile" inflammation in both periphery and brain independently of the noncanonical caspase-11 inflammasome. Ablation of Nlrp3 inflammasome protected mice from age-related increases in the innate immune activation, alterations in CNS transcriptome, and astrogliosis. Consistent with the hypothesis that systemic low-grade inflammation promotes age-related degenerative changes, the deficient Nlrp3 inflammasome-mediated caspase-1 activity improved glycemic control and attenuated bone loss and thymic demise. Notably, IL-1 mediated only Nlrp3 inflammasome-dependent improvement in cognitive function and motor performance in aged mice. These studies reveal Nlrp3 inflammasome as an upstream target that controls age-related inflammation and offer an innovative therapeutic strategy to lower Nlrp3 activity to delay multiple age-related chronic diseases.

INTRODUCTION

The Nlrp3 inflammasome is unique among innate immune sensors, as it can be activated in response to a diverse array of endogenous metabolic "danger signals" to induce sterile inflammation in absence of overt infection (Dinarello, 2009; Martinon et al., 2009; Strowig et al., 2012). The Nlrp3 inflammasome controls caspase-1 activation, which is required for secretion of IL-1β and IL-18 to regulate obesity-induced inflammation and insulin resistance (Stienstra et al., 2011, Vandanmagsar et al., 2011; Wen et al., 2011). Clinically, aging is associated with increases in IL-18, IL-1 receptor antagonist (IL-1RA), and IL-6, while circulating IL-1β levels are undetectable (Ferrucci et al., 2005; Franceschi et al., 2007; Dinarello, 2009). Global age-related systemic inflammation in multiple organs, including adipose tissue and CNS, is postulated to be a common mechanism leading to several chronic degenerative disorders that negatively impacts the healthspan of the elderly (Lumeng et al., 2011; Green et al., 2011; Ferrucci et al., 2005; Franceschi et al., 2007). However, the mechanisms underlying maladaptive systemic inflammation in several organs in the absence of overt infection, as observed during aging, are still speculative.

Both IL-1β and IL-18 mediate several downstream effects of Nlrp3 inflammasome-dependent caspase-1 activation (Martinon et al., 2009). However, IL-1 is thought to play a predominant role in development of several age-related degenerative diseases, including type 2 diabetes and Alzheimer's disease (Youm et al., 2011; Heneka et al., 2013). Importantly, in addition to IL-1, caspase-1 has multiple substrates and can also induce adipose tissue inflammation and insulin resistance by cleavage of Sirt1 (Chalkiadaki and Guarente., 2012). Depending on the disease model, several redundant upstream mechanisms control the processing and secretion of mature IL-1β; these include neutrophil-derived serine proteinase 3 and granzyme A (Dinarello, 2009). In addition to distinct NLR and AIM2 inflammasomes, caspase-1 can also be activated via CARD-CARD interactions of the noncanonical caspase-11 inflammasome in response to pathogens (Kayagaki et al., 2011; Strowig et al., 2012). Notably, the Nlrp3 inflammasome can also be activated by nonmicrobial origin DAMPs such as lipotoxic fatty acids (Wen et al., 2011), ceramides (Vandanmagsar et al., 2011, Youm et al., 2012), free cholesterol (Duewell et al., 2010; Youm et al., 2012), uric acid (Martinon et al., 2006), ATP (Mariathasan et al., 2006), and ROS (Strowig et al., 2012). Many DAMPs are elevated during aging and thus could trigger Nlrp3 inflammasome activation to produce age-related inflammation (Ruggiero et al., 2006; Cutler et al., 2004).

Age-related inflammation in multiple organs may lead to functional decline even in absence of a specific disease. It has been hypothesized that fundamental trade-off between the

cost-benefit ratio of inflammatory immune response that allows survival against early life infections may have deleterious consequences on organ function as human lifespan extends beyond the reproductive age in a constructed niche of energy excess and relatively low microbial exposure (Okin and Medzhitov 2012). Notably, aging remains a significant risk factor for multiple chronic diseases such as diabetes, atherosclerosis, dementia, arthritis, and cancer (Green et al., 2011). However, the identity of immune sensors that mediate a chronic inflammatory state in normal aging process remains obscure, and it is also uncertain whether reduction in specific proinflammatory mechanisms can impact the multiple degenerative conditions during aging. Here, we show that the Nlrp3 inflammasome is a major sensor of age-related accumulation of DAMPs and an upstream regulator that controls caspase-1-mediated proinflammatory state in aging independently of caspase-11 pathway. Consistent with the long-held belief that low-grade chronic inflammation instigates age-related functional decline, we present experimental evidence to support the hypothesis that reduction of Nlrp3 inflammasome is a common mechanism that extends the healthspan and attenuates multiple age-related degenerative changes in periphery as well as brain. In addition, we show that during aging, IL-1 signaling does not mediate Nlrp3 inflammasome effects on glucose tolerance, thymic demise, T cell senescence, and bone loss. Our data reveal that IL-1 regulates Nlrp3-mediated cognitive decline and functional measures of frailty. These data provide evidence that inhibiting aberrant Nlrp3 activity during aging may lower age-related chronic diseases driven by inflammation.

RESULTS

The Nlrp3 Inflammasome Controls Age-Related Inflammation in Periphery

Recent evidence suggests that in response to high-fat diet (HFD), Nlrp3- and Asc-deficient mice defend against adiposity (Stienstra et al., 2011). However, it has also been demonstrated that development of HFD-induced dysbiosis in a different strain of Asc mutant mice causes increased obesity (Henao-Mejia et al., 2012). Therefore, we monitored the body weight of normal chow-fed *Nlrp3*$^{-/-}$ and *Asc*$^{-/-}$ mice until 24 months of age. When fed a normal chow diet, the *Nlrp3*$^{-/-}$ *and Asc*$^{-/-}$ mice did not show any significant difference in body weight until 6 months of age. However, the male *Nlrp3*$^{-/-}$ mice weighed significantly more than WT and *Asc*$^{-/-}$ mice at 9 and 20 months of age (Figures S1A and S1B). By 24 months of age, male and female Nlrp3, Asc, and caspase-11 mutant mice did not show any significant difference in body weight (Figures S1A and S1B). Furthermore, compared to 24-month-old WT mice, the *Nlrp3*$^{-/-}$ animals did not show any difference in body composition (Figure S2) or hepatic steatosis (Figure S1B), and no change in hepatic *Il6* was detected (Figure S2B).

Nlrp3 inflammasomes can sense a wide array of DAMPs; indeed, multiple age-relevant DAMPs such as extracellular ATP, urate, ceramides, and palmitate induced IL-1β activation in macrophages in an Nlrp3-dependent manner (Figure 1A). Furthermore, ablation of Nlrp3 lowered aging-associated caspase-1 activation in adipose tissue (Figure 1B, Figure S1C), suggesting reduction in inflammasome-dependent peripheral inflammation. Further investigation revealed that age-related increase in adipose tissue IL-1β expression was significantly reduced in Nlrp3-deficient mice but not in aged caspase-11 mutants, while no significant age-related changes were detected in liver (Figure 1C).

Interestingly, age-related increase in circulating IL-18 was significantly reduced in Nlrp3-deficient mice (Figure 1D) and was unaffected in *Casp11*$^{-/-}$ mice, whereas the loss of Asc totally abrogated the rise of IL-18 in aged mice (Figure 1D). Given that Asc is also required for the assembly of Nlrp6, Nlrp12, and AIM2 (absent in melanoma2) inflammasome (Strowig et al., 2012), these data suggest that multiple inflammasomes may partake in mechanisms that control age-related rise in IL-18. Serum and plasma IL-1β levels in 23-month-old WT mice were not measurable. Furthermore, the loss of Nlrp3 and Asc did not affect the age-related increase in IL-6 (Figure 1E). Given that development of age-related inflammation is linked to glucose intolerance, and Nlrp3-deficient mice are protected from age-related increase in caspase-1 activation, we conducted glucose tolerance tests at 14, 19, and 23 months of age in three different cohorts of mice (Figures 1F and 1G). Compared to 19- and 23-month-old WT mice (Figure 1G), the Nlrp3 mutant animals displayed improved glucose tolerance, while no change in GTT was observed at 14 months of age (Figure 1F).

During obesity, IL-1β mediates the majority of downstream effects of Nlrp3 inflammasome activation that produce glucose intolerance (Stienstra et al., 2011; McGillicuddy et al., 2011). Therefore, we next evaluated the role of IL-1 in development of glucose intolerance during healthy aging process. Similar to *Nlrp3*$^{-/-}$, the aged *Il1r*−/− mice did not show increased adiposity or alteration in lean or fat mass (Figure S2C). We found that ablation of IL1 signaling in aged mice reduced the proinflammatory complement component C3 (Figure 1H) without affecting *Tnf* and *Il10* gene expression (Figures 1I and 1J). Furthermore, in contrast to diet-induced obesity (Stienstra et al., 2011; McGillicuddy et al., 2011), the 20-month-old chow-fed *Il1r*−/− mice did not show any improvement in glucose tolerance when compared to WT controls (Figure 1K). Notably, caspase-1 activation impairs lipid metabolism independently of IL-1 and IL-18 family of cytokines (Kotas et al., 2013). Our data suggest that during aging, reduction in Nlrp3 inflammasome-induced caspase-1 activation improves glucose tolerance independently of IL-1.

Given that the expansion of effector T cells at the expense of naive cells is a hallmark feature of peripheral inflammation that is linked to thymic involution (Goronzy and Weyand, 2005), we next examined the role of canonical Nlrp3 inflammasome, caspase-11, and IL-1 on thymic aging and effector T cells during aging. The aging cohorts of Nlrp3-deficient mice were significantly protected from age-related thymic involution as evidenced by reduced ectopic adipocytes, increased thymic size, and maintenance of cortical and medullary architecture and increased thymic mass and thymocyte numbers (Figure 2A).

The ablation of inflammasome adaptor, Asc, significantly reduced age-related effector T cell expansion with higher naive T cell frequency in spleen while the aged caspase-11 mice were indistinguishable from the WT mice (Figures 2B and 2C). Importantly, recent data suggest that loss of Dock2 expression due to potential inactivating passenger mutations in certain strains of Asc-deficient mice causes alterations in T cell homeostasis, which results in lower naive T cell frequency (Ippagunta et al., 2011). Given that our Asc-deficient mice had higher naive

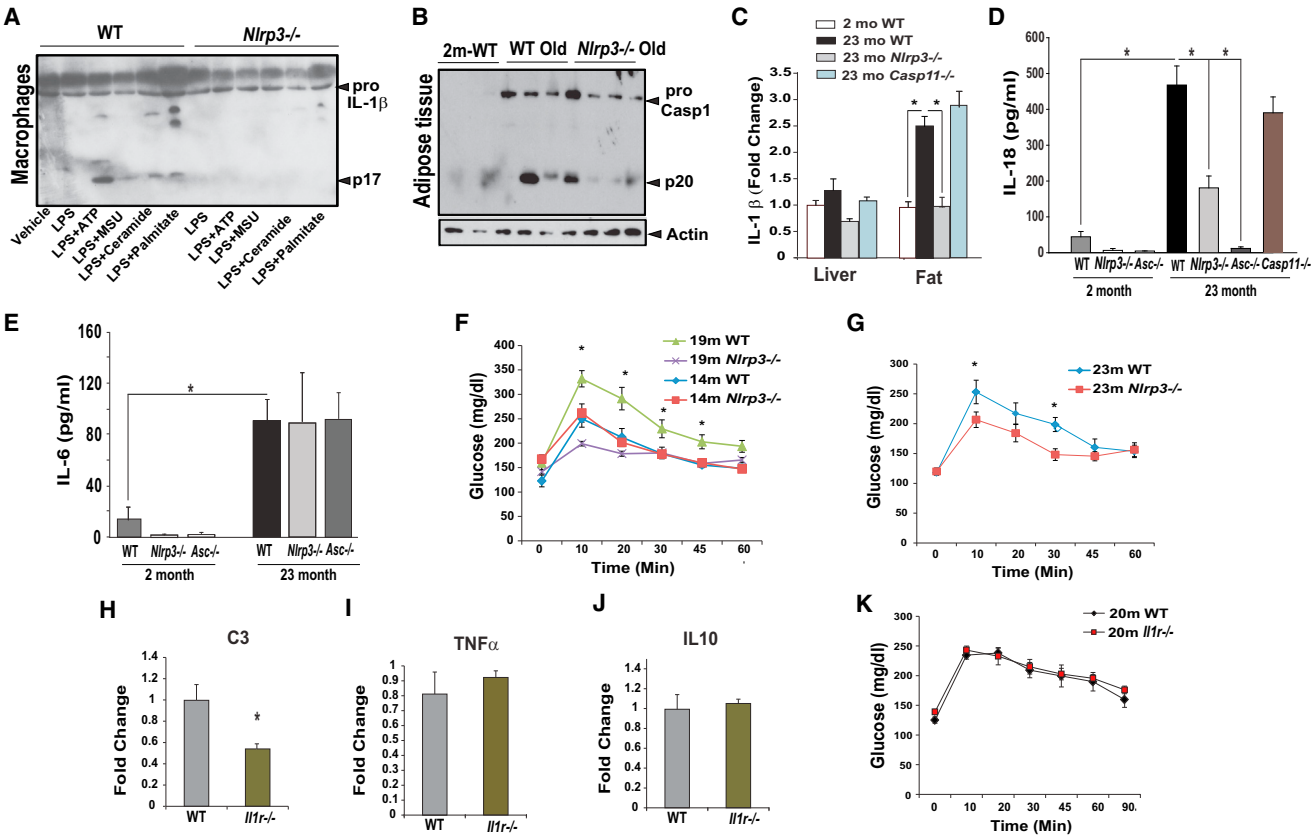

Figure 1. The Nlrp3 Inflammasome Controls Metabolic Inflammation and Glucose Intolerance in Aging

(A) LPS primed WT and *Nlrp3*$^{-/-}$ BMDMs were stimulated with multiple aging-relevant DAMPs, and supernatants were analyzed for active IL-1β (p17) by immunoblotting.

(B) Caspase-1 immunoblot analysis in epididymal adipose tissue of 2- and 15-month-old WT and 15-month-old *Nlrp3*$^{-/-}$ mice maintained on control chow diet. Age-related increase in caspase-1 activation (p20) subunit of caspase-1 is substantially reduced in absence of Nlrp3.

(C) Real-time PCR analysis of proinflammatory cytokines *Il1b* in liver and epididymal fat pad (n = 4–6/age group/genotype).

(D and E) Serum IL-18 (D) and IL-6 (E) levels in 2- and 23-month-old WT, *Nlrp3*$^{-/-}$ and *Asc*$^{-/-}$, *Casp11*$^{-/-}$ mice (n = 6–8 mice per age group/strain).

(F and G) Glucose tolerance test in 14- and 19- (F) and 23-month-old (G) WT, *Nlrp3*$^{-/-}$ mice maintained on control chow diet (n = 7–9/age group/genotype).

(H–K) Real-time PCR analysis of proinflamamtory mediators complement *C3*, *Tnf*, and *Il10* in epididymal adipose tissue (H–J) and glucose tolerance test (K) in 20-month-old WT and *Il1r*$^{-/-}$ mice (n = 9/group). All data are presented as mean (SEM) *p < 0.05. See also Figures S1 and S2.

T cell frequency, we examined the Dock2 expression in spleen and bone-marrow-derived macrophages of aged WT and *Asc*$^{-/-}$ mice. We found that Asc-deficient mice in our colony express Dock2 normally, and protection from inflammation-induced degenerative changes in aged *Asc*$^{-/-}$ mice is not dependent on Dock2 mutation or dysregulation (Figure 2D). Interestingly, unlike Nlrp3- and Asc-deficient mice, loss of IL-1 signaling in aged animals did not protect against thymic demise (Figures 2E and 2F). Compared to 20-month-old WT mice, the *Il1r*−/− mice did not show any change in thymic weight or thymocyte numbers (Figure 2E) and CD4 and CD8 naive and effector T cell frequency (Figure 2F).

The Nlrp3 Inflammasome Induces Age-Related Hippocampal Astrogliosis and Inflammation in CNS

Age-related inflammation is thought to negatively impact CNS function. Furthermore, considering that the inflammasome is expressed in myeloid lineage cells, and microglial activation is implicated in causing age-related dementias (Cutler et al., 2004; Czirr and Wyss-Coray, 2012; Ransohoff and Brown, 2012), we next asked whether the canonical Nlrp3 inflammasome regulates inflammation in aging brain. No differences in inflammasome-dependent alterations in hippocampal microglial distribution were observed in aged mice (Figure S3A). Immunostaining with Iba1^{+} revealed that ablation of Nlrp3 in 23-month-old mice reduced the microglial activation in the dentate gyrus (DG) region of hippocampus (Figure 3A). Consistent with reduced microglial activation, the ablation of both *Nlrp3* and *Asc* significantly reduced mRNA expression of proinflammatory cytokines *Il1b* and *Tnf* (Figures 3B and 3C) without significantly affecting the age-related increase in *Il6* in hippocampus (Figure S3B). Interestingly, ablation of Nlrp3 did not protect against age-related increase in hypothalamic microglial activation (Figure S4A) and inflammation (Figure S4B), suggesting specific effects on the brain regions that control cognition and memory.

Astrogliosis is an important mechanism that contributes to age-related functional decline and dementia (Ransohoff and Brown, 2012). The GFAP staining revealed reduced astrogliosis

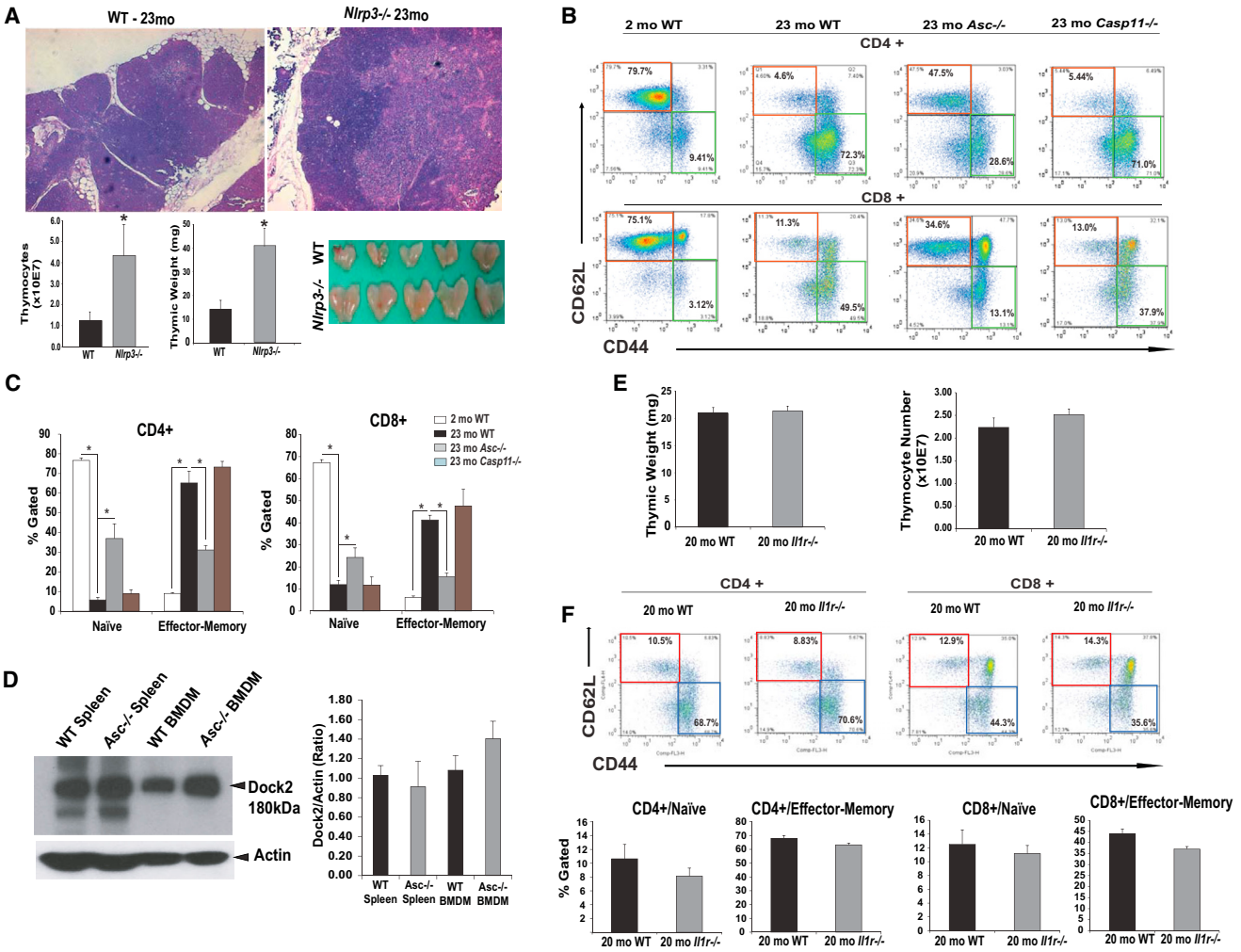

Figure 2. Ablation of Nlrp3 Inflammasome Reduces Age-Related Thymic Involution and Effector T Cell Expansion in an IL-1-Independent Mechanism

(A) Thymi of 23-month-old WT and Nlrp3 mice. The FFPE section of 23-month-old *Nlrp3*$^{-/-}$ mice display reduced ectopic lipid, maintenance of cortical-medullary junctions, and lower thymic involution as measured by increased thymic mass and total thymocyte counts in Nlrp3 mutant mice.

(B and C) FACS analysis depicting (CD4/CD8^{+}CD62L^{+}CD44^{-}) and effector-memory E/M (CD4/CD8^{+}CD62L^{-}CD44^{+}) T cells from 2- (left) and 23-month-old (right) WT and age-matched *Asc*$^{-/-}$ and *Casp11*$^{-/-}$ mice (n = 6–8).

(D) Immunoblot analyses and quantification of dock2 in spleen and bone-marrow-derived macrophages (BMDMs) of WT and *Asc*$^{-/-}$ mice.

(E) Thymic weight and total thymocyte counts for 20-month-old WT and *Il1r*$^{-/-}$ mice (n = 9/group).

(F) The FACS analysis of splenocytes revealed that compared to 20-month-old WT mice, the *Il1r*$^{-/-}$ mice do not show any significant difference in CD4 or CD8 naive and effector-memory frequency (n = 9/group). All data are presented as mean (SEM) *p < 0.05.

in hippocampus of aged *Nlrp3*$^{-/-}$ mice (Figure 3D). Interestingly, the age-related increase in GFAP immunostaining that localized to the DG region was lower in age-matched Nlrp3 mutants (Figure 3D). To further confirm a role of the inflammasome in astrogliosis, we placed WT and *Nlrp3*$^{-/-}$ mice on HFD for a period of 14 months and then examined the GFAP immunopositivity (Figure S3C). Obesity significantly accelerates astrogliosis and age-related neurodegeneration (Frisardi et al., 2010, Czirr and Wyss-Coray 2012); importantly, we found that HFD- and aging-induced hippocampal astrogliosis was reduced in *Nlrp3*$^{-/-}$ mice (Figures S3C and 3F). In addition, purified Glast1^{+} astroglial cells express high levels of procaspase-1 and in response to extracellular ATP are fully competent to induce inflammasome activation (Figure 3G). Further examination of astrocyte morphology by GFAP staining revealed that in DG regions, aged WT mice displayed astrocyte hypertrophy (Figure 3E). Consistent with increased age-related astrogliosis, the PoDG and Mol layer of DG in aged WT mice displayed pronounced overlap of astrocyte processes (Figure 3E). Interestingly, in age-matched *Nlrp3*$^{-/-}$ mice, astrocytic hypertrophy was reduced and the territories of astrocyte processes did not overlap, suggesting reduced astrogliosis (Figure 3E). Importantly, the investigation of caspase-1 activation in CNS revealed that elimination of Nlrp3 substantially reduced the age-related increase in caspase-1 cleavage (Figures 3H and 3I) as well as activated the p17 subunit of IL-1β in hippocampus (Figure 3J and Figure S3D).

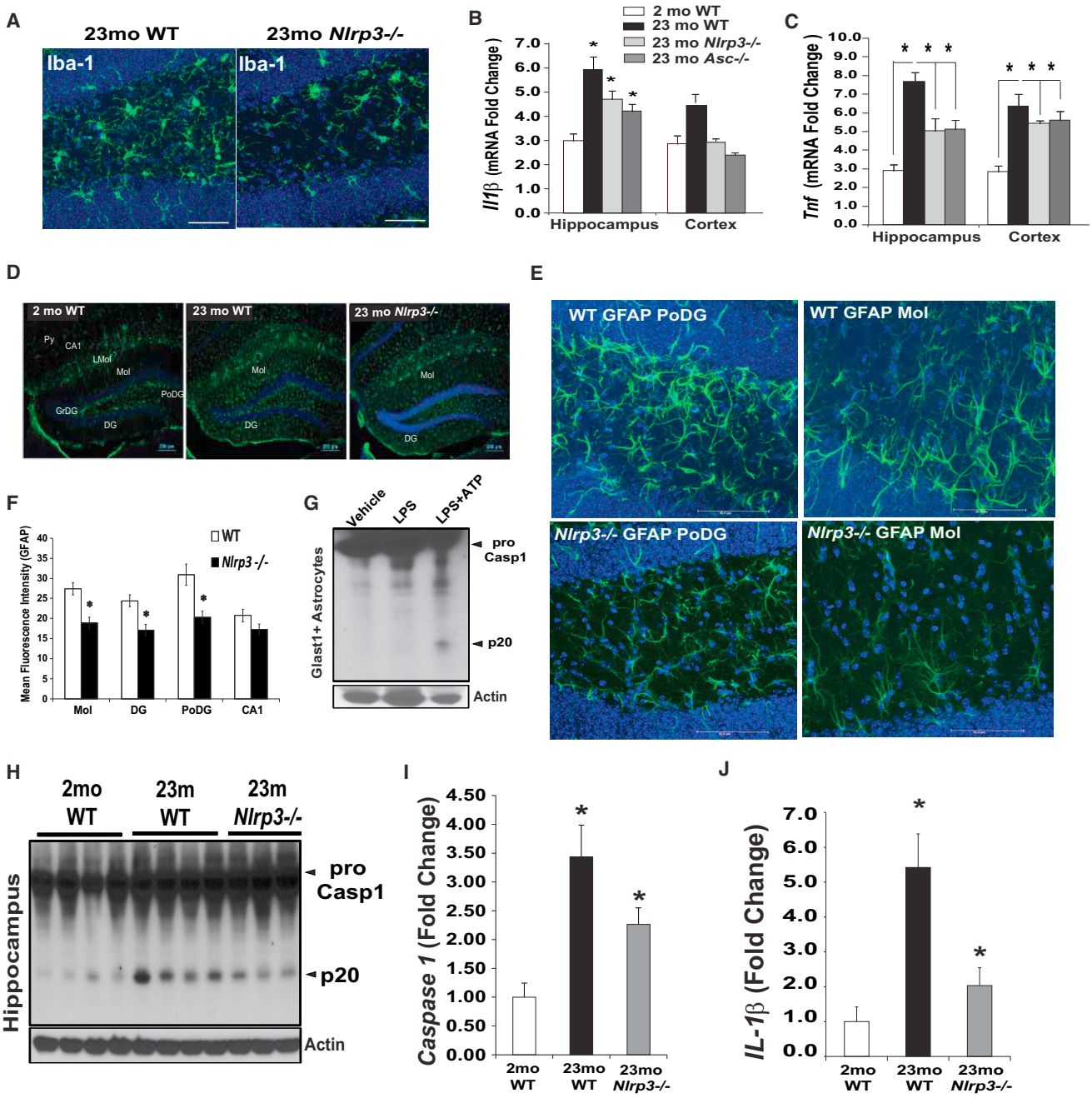

Figure 3. Nlrp3 Inflammasome Regulates Age-Related Caspase-1 Activation and Astrogliosis in Brain

(A) Brain cryosections from WT and Nlrp3 mutant mice (23 months old) were stained with anti-Iba antibody Alexa Fluor 488 (green) to identify microglial morphology in dentate gyrus region of hippocampus. Representative confocal Z stack images revealed reduced microglia activation in aged *Nlrp3*$^{-/-}$ mice (n = 5).

(B and C) Real-time PCR analysis of proinflammatory cytokines *Il1b* (B) and *Tnf* (C) in hippocampus and cerebral cortex in young (2 months) and old (23 months) WT, *Nlrp3*$^{-/-}$, and *Asc*$^{-/-}$ mice (n = 4–6 per age group/strain).

(D) Brain cryosections from WT and *Nlrp3*$^{-/-}$ mice (23 months old) were stained with anti-GFAP antibody. Hippocampal astrogliosis was evident in aged DG (dentate gyrus) and Mol (molecular layer of DG) while *Nlrp3*$^{-/-}$ mice displayed lower GFAP immunoreactivity in DG and regions.

(E) The confocal Z stack analysis of anti-GFAP-stained cryosection of 24-month-old WT and *Nlrp3*$^{-/-}$ mice in PoDG and Mol layer of hippocampus revealed that loss of Nlrp3 protects against age-related astrogliosis and change in astrocytic morphology (n = 4/strain repeated thrice).

(F) Quantification of mean fluorescence intensity of GFAP immunoreactivity in hippocampus of WT and *Nlrp3*$^{-/-}$ mice maintained on 60% HFD for 14 months.

(G) The caspase-1 immunoblot analysis of Glast1^{+} astrocytes primed with LPS and stimulated with ATP reveals the presence of active p20 subunit of capsase-1.

(H–J) Caspase-1 (H and I) and IL-1β (J) quantification by immunoblot analysis in hippocampus of 2-month-old and 23-month-old WT and 23-month-old *Nlrp3*$^{-/-}$ mice. All data are presented as mean (SEM) *p < 0.05. See also Figures S3 and S4.

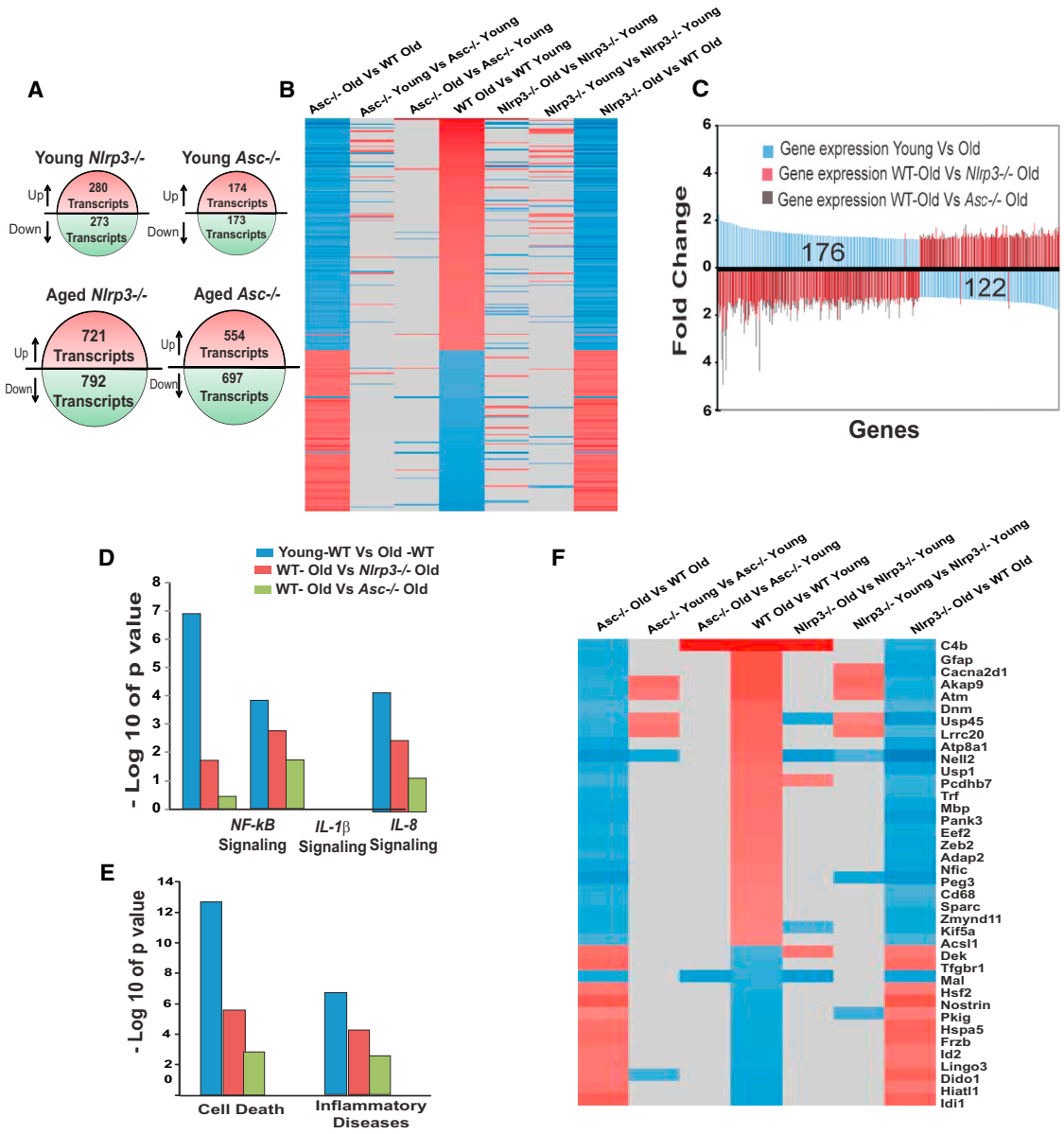

Figure 4. Nlrp3 Inflammasome Regulates Age-Dependent Alterations in Hippocampal Transcriptome

(A) The age-related changes in gene expression profiling on hippocampal tissue obtained from WT as well as Nlrp3 and Asc mutant mice.

(B) A set of 298 gene probes that respond to aging and are modulated by loss of Nlrp3 and Asc.

(C) Examination of the direction of change revealed that nearly all (295 of 298) gene probes with expression differences between old and young WT (blue bars) show expression changes in the opposite direction when comparing old mutant to old WT.

(D and E) Pathway analyses of genes with age-dependent expression differences reveal a strong enrichment of genes related to cell death as well as to inflammatory disease in WT mice compared to Nlrp3 and Asc mutants. Similar differences in association were found for NF-κB, IL-1, and IL-8 signaling, where the respective pathways were found to be strongly associated with age-dependent expression differences in WT mice compared to *Nlrp3*$^{-/-}$ *and Asc*$^{-/-}$ animals.

(F) The list of genes ($p < 0.05$, 1.5-fold change) that are involved in cell death and inflammation and regulated by both Nlrp3 and Asc during aging. This pattern suggests that these genes are characterized by age-dependent gene expression changes, which are regulated by the absence of the Nlrp3 inflammasome activity. See also Figure S5.

The Ablation of Nlrp3 Inflammasome Protects against Age-Related Alterations in the Transcriptome

To provide a more global view, we employed gene expression profiling to gain further understanding of the Nlrp3 inflammasome-dependent mechanism of age-related inflammation in hippocampus. Compared to young WT and mutant mice, we observed significantly broader expression differences in aged WT and *Nlrp3*$^{-/-}$ and *Asc*$^{-/-}$ mice (Figure 4A), involving 2.5–3 times more genes compared to young (Figure 4A). Genes were first queried for age-dependent expression changes in WT

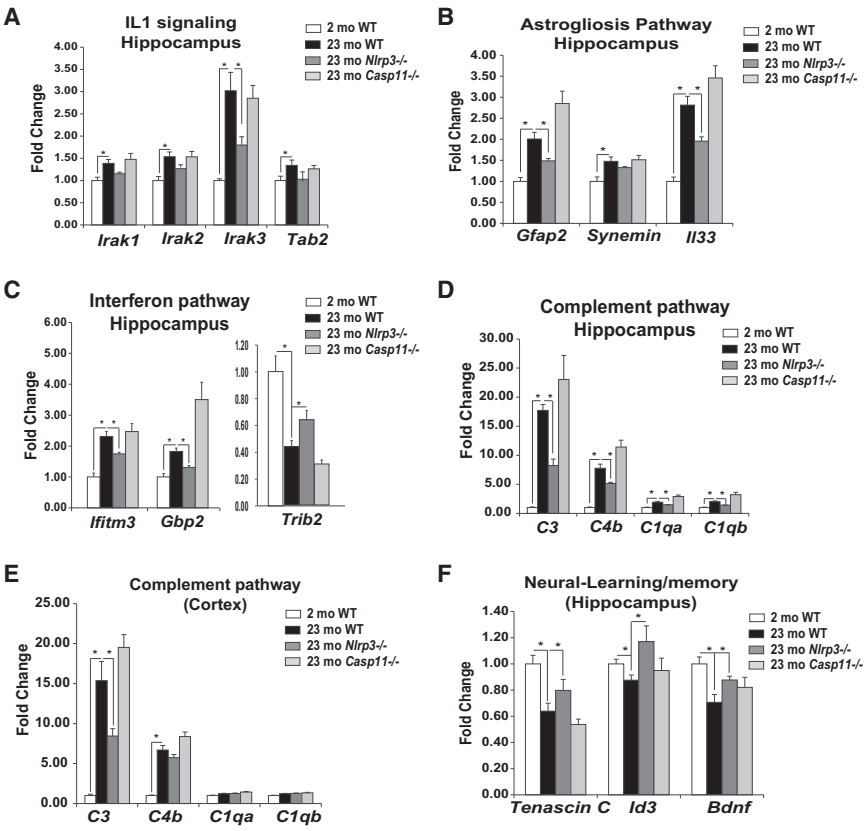

Figure 5. Ablation of Canonical Nlrp3 Inflammasome Reduces Innate Immune Activation in CNS

(A–E) The hippocampi from young, old WT, and old (23 months) *Nlrp3*$^{-/-}$ and *Casp11*$^{-/-}$ were used to confirm the pathways identified from microarray profiling. Real-time PCR analysis of (A) IL-1 signaling, (B) astrogliosis pathway, (C) interferon pathway and (D and E) complement pathway, and (F) gene implicated in cognitive function. All data are presented as mean (SEM) *p < 0.05.

mice. The resulting subset of genes was then interrogated for presence of genes with genotype-dependent changes of expression in old mice, with the goal of identifying pathways that are modulated by the loss of Nlrp3 inflammasome activity in aging (Figure 4B). Figure 4B shows the set of 298 gene probes that respond to aging, yet are modulated by either of the two mutant genotypes (Nlrp3 and Asc). The gene probes were sorted according to their expression change observed in the wild-type, old-versus-young comparison. Nearly all gene probes show reciprocal regulation when comparing age effects in WT to genotype effects in old mice, as genes with age-dependent increase of expression showed reduced expression in old Nlrp3- and Asc-deficient mice compared to old WT mice, and vice versa (Figure 4B). Comparing age-dependent changes in the mutants (aged *Asc*$^{-/-}$ versus young *Asc*$^{-/-}$, aged *Nlrp3*$^{-/-}$ versus young *Nlrp3*$^{-/-}$) to WT (young versus old) shows that only a small fraction of these gene probes respond to genotype in young mice (Figure 4B).

Comparing the age-dependent response in WT to genotype-dependent responses among aged animals, a total of 298 gene probes were impacted by ablation of both Nlrp3 and Asc (Figure S5). Interestingly, examination of the direction of change revealed that nearly all (295 of 298) gene probes altered with age in WT mice showed expression changes in the opposite direction when comparing both old Nlrp3 and Asc mutants to old WT mice (Figure 4C). Consistent with recent studies, our data revealed that age-associated enrichment of NF-κB, IL-1, and IL-8 signaling proinflammatory pathways was partially dependent on the Nlrp3 inflammasome (Figure 4D). Furthermore, gene ontology enrichment analysis revealed that ablation of the Nlrp3 inflammasome protected against age-related elevation of cell death and inflammation pathways (Figure 4E). The genes identified from these analyses suggest that the group of genes involved in cell death and inflammatory process are characterized by age-dependent gene expression changes that are moderated by the absence of both Asc and the Nlrp3 inflammasome activity (Figure 4F). Notably, in certain disease models Asc may have unique functions that are independent of inflammasome-mediated caspase-1 cleavage (Ippagunta et al., 2011). Our data provide evidence that during aging, Nlrp3 and Asc perform analogous, Nlrp3 inflammasome-dependent functions to regulate age-related inflammation.

Reduction in Canonical Nlrp3 Inflammasome Reduces Age-Associated Innate Immune Activation

We next investigated the age-dependent and Nlrp3 inflammasome-regulated pathways that were identified from the global expression profiling analysis in hippocampus. Consistent with a role of IL-1β signaling in mediating Nlrp3 inflammasome downstream effects, age-related increases in *Irak3* mRNA were significantly reduced in hippocampus of aged Nlrp3 null mutants (Figure 5A). The astrogliosis signatures identified from microarray in hippocampus confirmed that age-related increases in *Gfap* and alarmin *Il33* expression were dependent on Nlrp3 without affecting synemin (Figure 5B). Ablation of Nlrp3 protected against age-related activation of interferon response (*Ifitm3*, *Gbp2*, and *Trib2*) in hippocampus (Figure 5C). We identified marked age-related increases in complement pathway genes—*C3*, *C4*, *C1qa*, *C1qb*—in hippocampus (Figure 5D) as well as cortex (Figure 5E), which were significantly reduced in Nlrp3-deficient mice. Reduction in Nlrp3 inflammasome hippocampus was associated with increases in genes involved in learning and memory (*Tenascin*, *Id3*, and *Bdnf*) (Figure 5F). Interestingly, ablation of noncanonical caspase-11 inflammasome did not protect against age-related gene expression changes observed in hippocampus or cortex (Figures 5A–5F).

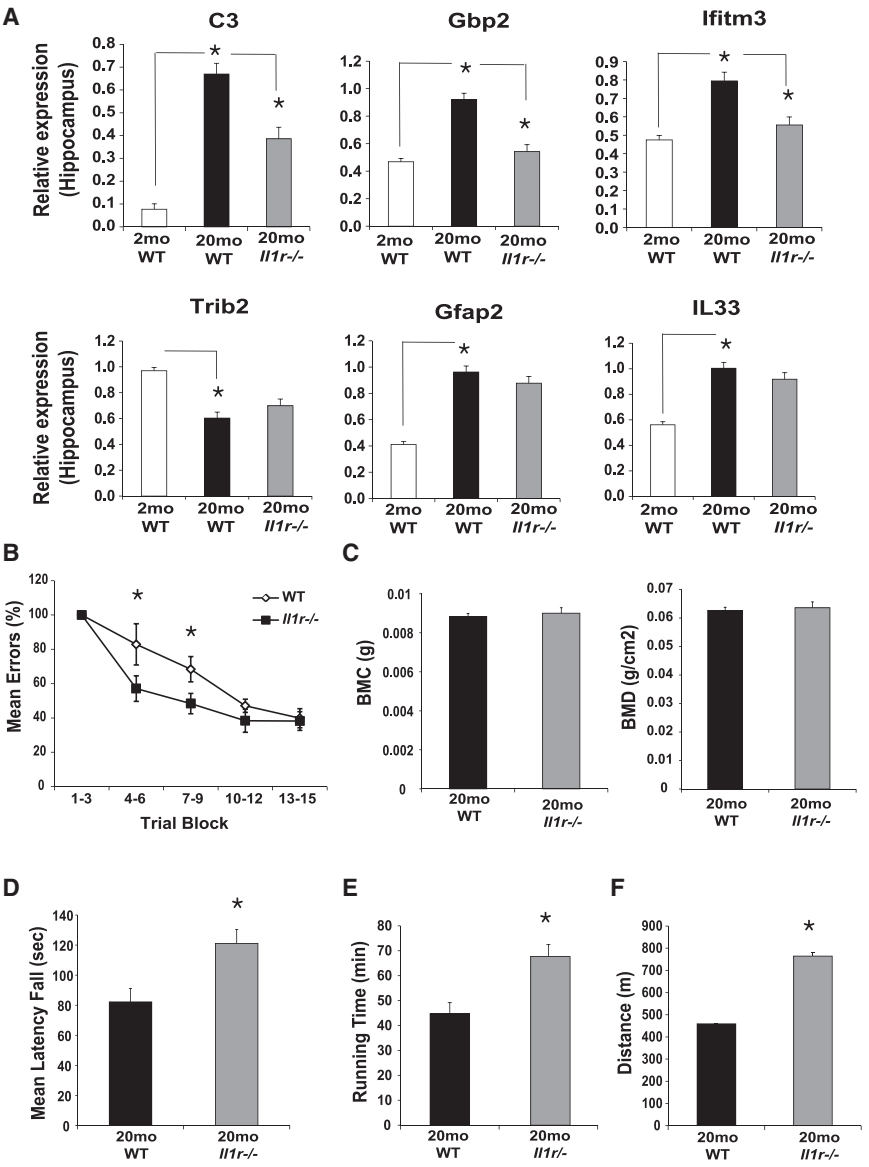

Figure 6. Ablation of IL-1 Signaling Partially Protects against Age-Related Functional Decline

(A) The hippocampi from separate cohort of young (3 months), old (20 months) WT, and *Il1r*$^{-/-}$ mice (n = 6–12/group) were analyzed for complement, interferon, and Nlrp3-dependent inflammatory genes using real-time PCR.

(B) The Stone T-maze test in 20-month-old WT mice and age-matched *Il1r*$^{-/-}$ mice (n = 12/group). Mice were given 15 trials in the T-maze with each trial having a maximum length of 300 s, and the number of errors during each trial block was recorded.

(C) Bone mineral content of femorae of 20-month-old WT and *Il1r*$^{-/-}$ mice (n = 12) is measured in grams of calcium hydroxypatite; bone mineral density represents the mineral in bone per area, i.e., areal bone mineral density.

(D) The mean latency to fall from a rotating rod (rotarod test) in 20-month-old WT and *Il1r*$^{-/-}$ mice (n = 12).

(E and F) The treadmill test showing total running time and total distance run by 20-month-old WT and *Il1r*$^{-/-}$ mice (n = 12). All data are presented as mean (SEM) *p < 0.05.

IL-1 Partakes in Regulating Age-Related CNS Inflammation and Functional Decline

IL-1 signaling downstream of Nlrp3 inflammasome activation is hypothesized to be a major mechanism that controls "sterile" inflammation in CNS and in several age-related chronic diseases including dementia (Dinarello, 2009; Martinon et al., 2009; Strowig et al., 2012). We found that, similar to the hippocampi of aged Nlrp3-deficient mice, the age-related increases in complement *C3* and interferon response genes *Gbp2* and *Ifitm3* were blunted in aged IL-1 receptor null mice (Figure 6A). However, unlike *Nlrp3*$^{-/-}$ mice, the disruption of IL-1 signaling in aging did not affect age- and Nlrp3-dependent inflammatory markers *Trib2*, *Gfap*, and *Il33* (Figure 6A). Next, we utilized the Stone T-maze test to evaluate age-related changes in memory and learning because this test avoids the confounding effects of impaired visual function seen in old mice (Pistell et al., 2012). Importantly, and consistent with overall reduction in inflammation in hippocampus, analysis of cognitive function, one of the measures of functional decline, revealed that, compared to WT mice, the aged *Il1r*−/− animals displayed partially improved learning ability in a Stone T-maze (Figure 6B).

Given that age-related inflammation is linked with other degenerative changes, such as reduced bone mass and increased frailty, we also investigated the motor performance measured on the rotarod and the treadmill tests. Analysis of bone mineral content and bone mineral density of femurs revealed no difference between *Il1r*−/− animals and the 20-month-old WT controls (Figure 6C). Interestingly, compared to WT mice, the 20-month-old IL-1R-deficient animals displayed enhanced performance on the rotarod (Figure 6D) and displayed significantly increased running time and distance on the treadmill (Figures 6E and 6F), suggesting reduced frailty.

Reduction in Nlrp3 Inflammasome Activity Extends Healthspan

As further evidence that reduction of Nlrp3 inflammasome activity links inflammation with age-related functional decline, we noted remarkable effects on several age-sensitive functional and pathological indices. Consistent with significant reduction in hippocampal inflammation and astrogliosis, the aged *Nlrp3*$^{-/-}$ mice were significantly protected from age-related decline in cognition and memory (Figure 7A). Importantly, error performance of WT and *Nlrp3*$^{-/-}$ mice during the first two blocks of maze training did not differ significantly (Figure 7A). These data demonstrate that the performance requirements of the task were equivalent.

As additional support of this point, further analyses showed that *Nlrp3*$^{-/-}$ mice were actually "slower" in the maze over this same period (Figure 7B), opposite to what would be predicted if differences in enhanced motor performance of Nlrp3 mutants confounded the interpretation of cognitive differences. To further confirm this effect, an additional cohort of WT and mutant mice were aged until 24 months, at which time results show reduced numbers of errors made during maze acquisition in the older *Nlrp3*$^{-/-}$ mice (Figure 7C). No significant genotype effects were observed in open field and fear conditioning tests (Figures S6A and S6B). As further evidence that specific reduction in activation of the canonical Nlrp3 inflammasome activation, but not the caspase-11 inflammasome, drives many aging processes, aged caspase-11 null mice did not show any protection from age-related functional decline on rotarod or Stone T-maze test (Figures S6C and S6D).

Similar to *Il1r*−/− animals, the 18- and 24-month-old Nlrp3-deficient animals displayed enhanced performance on the rotarod (Figure 7D) and displayed significantly increased running time and distance on the treadmill (Figures 7E and 7F). Regarding age-sensitive pathological indices, aged Nlrp3 mutants displayed significantly reduced cataract formation (Figure 7G). Interestingly, unlike aged IL-1R-deficient animals, which were not protected from bone loss, the 24-month-old Nlrp3-deficient mice had significantly increased cortical (Figures 7H and 7I) and trabecular bone thickness (Figures 7J and 7K). As further evidence that reduction in Nlrp3 inflammasome activation protects against age-related bone loss, the 24-month-old *Nlrp3*$^{-/-}$ mice had significantly higher bone mineral content, bone mineral density, and total bone area (Figures 7L–7N). Aged *Nlrp3*$^{-/-}$ mice also exhibited greater cortical bone area (Figure 7O), as well as a higher polar moment of inertia (Figure 7P and Figures S6E–S6G), as a functional measure of greater bone strength. No reduction in marrow volume in aged Nlrp3-deficient mice was detected, an important observation that rules out development of osteopetrosis due to dysfunctional osteoclast activity (Figures S6H and S6I). Furthermore, in support of prior data that aging does not engage noncanonical inflammasome, the aged *Casp11*$^{-/-}$ mice were not protected from age-related changes in cortical or trabecular bone mass and mineral density (Figure S7). In summary, these data demonstrate that specific inhibition of Nlrp3 inflammasome-mediated caspase-1 activation controls age-related functional decline, and IL-1 proinflammatory cascade is not the sole mediator of downstream effects of Nlrp3 inflammasome activation during aging.

DISCUSSION

The mouse and human genome encodes 34 and 23 NLR (Nod-like receptor) family members, which can assemble into the inflammasome complex through homotypic protein-protein interactions (Martinon et al., 2009). It is currently not known whether age-related inflammation and inflammasome activation are regulated by specific NLRs. Importantly, Nlrp3 is unique among NLRs as it can sense a wide array of structurally diverse DAMPs, and excessive Nlrp3 inflammasome activation has been implicated in chronic diseases such as Alzheimer's diseases (Heneka et al., 2013), diabetes (Masters et al., 2010; Vandanmagsar et al., 2011; Wen et al., 2011; Youm et al., 2011), atherosclerosis (Duewell et al., 2010), arthritis, and gout (Martinon et al., 2006). That age is a common factor in development of all of the above chronic diseases raised several questions. First, is the IL-1β- and IL-18-driven chronic inflammation during the healthy aging process in the absence of overt diseases regulated by canonical or noncanonical inflammasome pathway? Second, is IL-1 signaling downstream of inflammasomes the major mechanism that controls age-related functional decline? This question has important translational implications in aging, because if IL-1β is a common trigger for age-related inflammation, it may be more efficient to use currently available IL-1 inhibitors instead of targeting multiple upstream inflammasomes and non-inflammasome-dependent mechanisms that control IL-1activation. Third, the "inflammaging theory" posits that "aging either physiologically or pathologically can be driven by the proinflammatory cytokines and substances produced by the innate immune system" (Franceschi et al., 2000; Goto., 2008). If the "inflammaging theory" is correct, one should predict that an experimental manipulation of a specific innate immune sensing pathway should result in attenuation of age-related functional decline across multiple systems. Our results provide compelling evidence that the Nlrp3 inflammasome activation causes global age-related inflammation in multiple organs, with consequences such as thymic demise, impaired glycemic control, reduced memory and cognition, motor performance, cataracts, and bone loss.

Given that aging-associated inflammation is systemic and the inflammasome is widely expressed in several organs, we examined age-related degenerative changes across multiple systems. Our data provide evidence that age-related increase in caspase-1 in adipose tissue, hippocampus, and thymus is partially controlled by the Nlrp3 inflammasome. Careful monitoring of body weight and composition of WT, *Nlrp3*$^{-/-}$, *Asc*$^{-/-}$, *Il1r*$^{-/-}$, and *Casp11*$^{-/-}$ animal cohorts maintained in SPF barrier and fed ad libitum normal chow diet revealed no significant change in adiposity at 24 months of age. Importantly, prior studies have shown that ablation of IL-18 induces hyperphagia, adiposity, and insulin resistance in mice, suggesting that IL-18 is required for improved glucose homeostasis (Netea et al., 2006). On the other hand, IL-1 is thought to play a predominant role in inducing insulin resistance in response to HFD (Stienstra et al., 2011; McGillicuddy et al., 2011). However, our studies revealed that during aging, in mice fed normal chow diet, IL-1 is not required for mediating downstream effects of Nlrp3 inflammasome on glucose intolerance. It is now known that caspase-1 acts on multiple substrates, including ones that control glycolysis (Shao et al., 2007) and Sirt1, which are relevant to aging and glucose homeostasis (Chalkiadaki and Guarente., 2012). Furthermore, caspase-1 is required for triglyceride clearance independently of IL-1 and IL-18 (Kotas et al., 2013). Importantly, our studies also revealed that improvement in insulin sensitivity in Nlrp3-deficient mice is relatively late in age and that initiation of insulin resistance is not a central event to development of degenerative disorders observed in aging. For example, aging of thymus precedes degenerative changes in many organs. Of note, the ablation of Nlrp3 protects against age-related thymic demise and restriction of T cell diversity before the emergence of metabolic dysfunction that appears in late life.

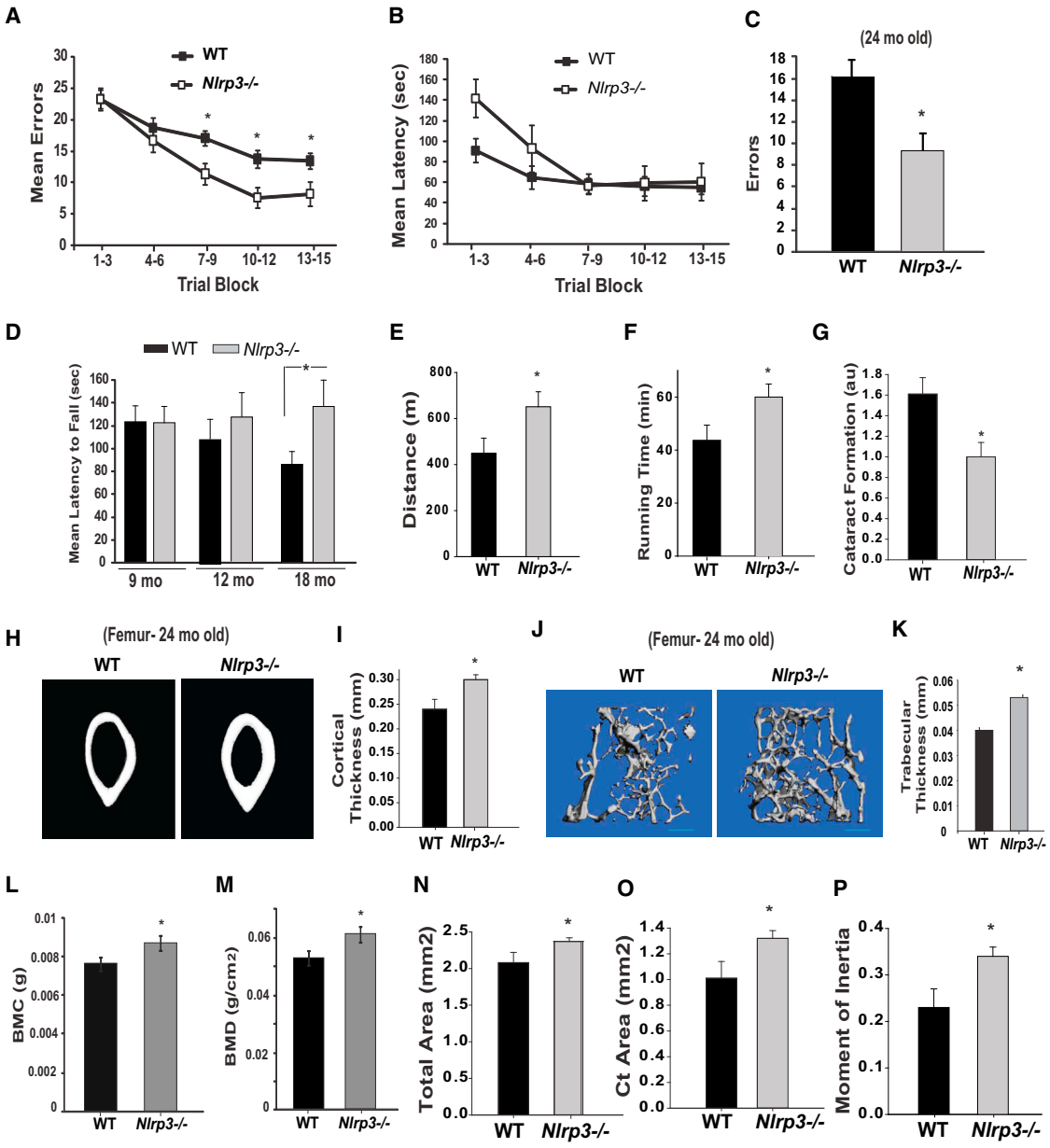

Figure 7. Reduction in Nlrp3 Inflammasome Activation Enhances Healthspan and Reduces Age-Related Functional Decline

(A) The Stone T-maze test in 18-month-old WT mice and age-matched *Nlrp3*$^{-/-}$ mice (n = 8/group). Mice were given 15 trials in the T-maze with each trial having a maximum length of 300 s. During each trial, the number of errors committed was recorded.

(B) Mean latency to reach the goal box during multiple trials of 18-month-old WT and *Nlrp3*$^{-/-}$ mice (n = 8/group).

(C) To confirm improved memory and cognitive performance, an additional cohort of WT littermates and *Nlrp3*$^{-/-}$ mice were aged for 24 months (n = 6–8/strain) and the total number of errors in a Stone T-maze test was recorded.

(D) Compared to WT mice, age-matched *Nlrp3*$^{-/-}$ mice (18 months old) displayed improved performance on the rotarod (tested in two separate cohorts of n = 8 each, 4 males and 4 females).

(E and F) At 24 months of age, additional old WT littermates and *Nlrp3*$^{-/-}$ mice were also tested for running distance and time using a treadmill test (n = 6–9/group) ($p = 0.05$).

(G) The same cohort of WT littermates and *Nlrp3*$^{-/-}$ mice were tested for lens opacity in both eyes by an ophthalmologist using a slit lamp and scored on a scale of normal (0), punctuate (1), incipient (2), diffuse (3), and complete (4). The ophthalmologist was blinded to the group identity to reduce investigator bias.

(H and I) Representative microcomputed tomographic images of cortical bone cross-sections from the mid-femur diaphysis of 24-month-old female WT (n = 5) and *Nlrp3*$^{-/-}$ mice (n = 8). The female WT and *Nlrp3*$^{-/-}$ mouse femurs were imaged by microcomputed tomography.

(J and K) The microcomputed tomographic scans of trabecular bone mass (J) and trabecular thickness (K) in 24-month-old male WT and *Nlrp3*$^{-/-}$ femorae.

(legend continued on next page)

The noncanonical caspase-11 inflammasome can interact with caspase-1 via the CARD domain (Wang et al., 1998). Also, caspase-11 and not caspase-1 is the major sensor of LPS and regulates endotoxemia-associated lethality in mice (Kayagaki et al., 2011). Importantly, recently work also shows that caspase-11 is a major sensor of LPS independently of TLR4, as priming of caspase-11 by sublethal dose of TLR3 agonists in *Tlr4*$^{-/-}$ mice and subsequent challenge of *Tlr4*$^{-/-}$ with LPS causes endotoxemia and morbidity (Kayagaki et al., 2013). Given that aging is associated with changes in gut microbiome (Claesson et al., 2012) and prior studies have reported circulating LPS as a potential cause of inflammation in metabolic syndrome (Creely et al., 2007), we also investigated if caspase-11 is involved in "inflammaging" process through potential interaction with gut-derived LPS. Our data further underscore the specificity of Nlrp3 inflammasome in causing "sterile" age-related inflammation without the engagement of caspase-11 by potential age-related "metabolic endotoxemia" caused by LPS leakage from GI tract.

Importantly, consistent with the "inflammaging theory," we found that reduction in Nlrp3 inflammasome-dependent proinflammatory cascade attenuated age-related degenerative changes across multiple organs. Prior studies have shown that astrogliosis is one of the mechanisms of age-related cognitive decline, and IL-1β is known to promote astrogliosis (Morgan et al., 1999). In the CNS, we found that the Nlrp3 inflammasome is a major regulator of age-related increase in caspase-1 and IL-1β. Importantly, reduction in Nlrp3 attenuated astrogliosis in hippocampus. Global gene expression analyses revealed that age-related activation of innate immune regulators, such as complement and interferon, was downregulated in Nlrp3 and Asc knockout mice. These data lend additional support to the recent evidence suggesting that complement activation promotes aging-related phenotypes (Naito et al., 2012). Consistent with our findings, treatment of acute onset demyelinating disorders in humans with IL-1 receptor antagonist Anakinra reduces complement C3 (Broderick et al., 2013). Our data demonstrate that IL-1 is required for Nlrp3 inflammasome-mediated age-related increase in complement C3 and interferon activation. Furthermore, IL-1 mediates in part the age-related reduction in cognitive function and motor performance, although the elimination of Nlrp3 led to greater protection from cognitive decline.

Notably, enhanced lifespan in mice treated with rapamycin is associated with amelioration of few aging phenotypes and also leads to several detrimental effects, such as increased cataract formation, testicular degeneration, and reduced insulin sensitivity (Lamming et al., 2012; Neff et al., 2013). Although it remains unknown whether reduction in Nlrp3 activation can extend lifespan, our data demonstrate unequivocally that deletion of Nlrp3 inflammasome enhances healthspan and prevents functional decline in multiple organs, including protection against thymic demise, cataract development, and glucose intolerance, and also enhances cortical and trabecular bone mass. Surprisingly, despite an important role of IL-1 in osteoarthritis (Dinarello, 2009), during the process of healthy aging, bone loss was dependent on Nlrp3 but independent of downstream IL-1 signaling. Interestingly, the increase in cortical bone mass has been demonstrated to be a predictor of enhanced lifespan in mice (Miller et al., 2011). Based on our findings, future studies will be required to test the hypothesis that attenuation of age-related degenerative changes mediated by Nlrp3 inflammasome promotes longevity.

In summary, activation of the Nlrp3 inflammasome in response to accumulation of various DAMPs induces systemic chronic inflammation in aging. Our data suggest that dietary or pharmacological approaches to dampen Nlrp3 inflammasome activation may be more efficient than targeting downstream cytokines in disrupting the feed-forward loop of inflammation and age-related chronic diseases.

EXPERIMENTAL PROCEDURES

Mice and Animal Care

The *Caspase11*$^{-/-}$, *Nlrp3*$^{-/-}$, and *Asc*$^{-/-}$ mice have been described (Mariathasan et al., 2006; Kayagaki et al., 2011). The *Il1r*$^{-/-}$ mice were purchased from Jackson Laboratories. All transgenic mice introduced in our colony were cross-fostered to our facilities with WT parent cohorts to minimize the confounding effects of alterations in microbiome. The WT littermates and mutant cohorts for aging studies were housed with a 12 hr light/12 hr dark cycle at 22°C. The mice were multi-housed and fed ad libitum normal chow diet consisting of 4.5% fat (5002; LabDiet) and aged in the specific pathogen-free barrier facility in ventilated cage racks that deliver HEPA filtered air to each cage with free access to sterile water through a hydropac system. Sentinel mice in our animal rooms were negative for currently tested standard murine pathogens (Ectromelia, EDIM, LCMV, *Mycoplasma pulmonis*, MHV, MNV, MPV, MVM, PVM, REO3, TMEV, and Sendai virus) at various times while the aging studies were performed (RADIL, Research Animal Diagnostic Laboratory, Columbia, MO). All experiments and animal use were conducted in compliance with the National Institutes of Health Guide for the Care and Use of Laboratory Animals and were approved by the Institutional Animal Care and Use Committee at Pennington Biomedical Research Center.

Antibodies

For FACS analysis the following antibodies (from eBiosciences, Inc.) were used: CD4-PerCP, CD8-APC, CD44-FITC, and CD62L-PE. All the FACS data were analyzed by postcollection compensation using FlowJo (Treestar, Inc.) software. The anti-GFAP and -Iba1 antibodies were from Cell Signaling. For western blot analysis: procaspase1 (p20 antibodies were from Genentech), IL-1β (actin antibodies were from R&D).

Rotarod Test and Stone T-Maze

This test is a widely used functional assay for measuring balance and coordination in rodents that has shown age-related sensitivity in mice. For the current study, the apparatus was manufactured by MED Associates (St. Albans, VT) and consists of a motor-driven cylinder with variable speed control. The rotarod begins moving at 4 rpm and over a period of 5 min accelerates to a speed of 40 rpm. The mouse is placed on top of the rotating cylinder at the slowest speed and permitted locomotion until falling (about 10 cm). The latency to fall from the rotarod is recorded. Each mouse received a total of five trials with readout recorded as mean time spent on the rotarod over five trials.

(L and M) Bone mineral content of 24-month-old male WT and *Nlrp3*$^{-/-}$ mice (n = 13) is measured in grams of calcium hydroxypatite; bone mineral density represents the mineral in bone per area, i.e., areal bone mineral density. The coefficient of variation for repetitive scanning ex vivo is approximately 2.4%.
(N–P) Similar to male mice, the 24-month-old female *Nlrp3*$^{-/-}$ mice displayed significant increase in (N) total bone area, (O) cortical area, and (P) moment of inertia (MOI). All behavioral and functional analyses in WT and mutant mice were conducted in an investigator-blinded fashion. All data are presented as mean (SEM) *p < 0.05. See also Figures S6 and S7.

The Stone T-maze test was performed as described previously (Pistell et al., 2012). Briefly, mice were required to navigate through a complex T-maze to reach a goal box as a test of cognition. Motivation to escape from the start box to the goal box involves the mouse wading through water (maintained at 21°C–24°C). During each trial, the number of errors committed and the latency to reach the goal box are recorded. The readouts for the assay are runtime and number of errors.

Treadmill Test

A Columbus Instruments' Eco 3/6 treadmill was used to analyze motor performance and endurance. The mice were motivated to run by an electric shock grid at the end of each lane. The mice were trained at a constant speed (8 m/min) for 20 min on 3 consecutive days prior to the test to allow proper acclimation (to the device) and avoid injury. On the day of the test, the speed was set to 8 m per minute, increasing 0.5 m every 5 min. The mice were allowed to run to exhaustion, which is after the third time the mouse is unwilling to return to the treadmill and remains on the shock grid. The latency to exhaustion was recorded for each mouse.

Microarray Analysis

The hippocampus from young (2 months, n = 4/genotype) and old (22 months, n = 6/genotype) WT, *Nlrp3*$^{-/-}$, and *Asc*$^{-/-}$ female animals were used to extract total RNA (RNAeasy, QIAGEN, Valencia, CA). Quality of RNA for array analysis was ascertained using an Agilent Bioanalyzer (Agilent Technologies, Santa Clara, CA). Biological replicates were amplified and labeled using the Epicenter TargetAmp Nano-g Biotin-aRNA Labeling Kit for the Illumina system. A total of 750 ng labeled RNA was hybridized to MouseRef-8 v2 BeadChip arrays (Illumina) according to the manufacturer's protocol. Array data were processed using Illumina GenomeStudio with respect to background subtraction and normalization. Data were initially filtered on p value of detection, with the requirement that gene probes either exhibit signal presence (i.e., $p < 0.05$) in all samples for a given pairwise comparison or show presence in all samples on one side of the comparative paradigm but not the other. Differential expression was assessed using CyberT using a t-statistic cutoff at $p < 0.05$ and a fold-change cutoff in either direction at 1.2-fold. Confirmatory pairwise and ANOVA analyses of data were performed in parallel with Geospiza GeneSifter as described before. JMP Genomics and Cluster3 were used for hierarchical clustering of genes with a significant difference ($-\log10(p) > 2.96$) in at least one experimental group as compared to the wild-type old group. Venn analysis was performed with JMP Genomics and gene ontology enrichment was performed using Ingenuity Pathway Analysis.

Cytokine Measurement

We measured the levels of IL-1β, IL-6 (eBioscience) bead assay, and IL-18 by ELISA (MBL, Japan) according to manufacturer's instructions.

Immunohistochemistry

Cryosections from formalin perfused brain were cut at 30 μm thickness on a sliding microtome. Free-floating sections were stained with anti-GFAP and anti-Iba1 antibodies, followed by fluorophore-conjugated secondary antibodies as described previously. Livers were formalin fixed, paraffin embedded, and stained with H&E. Nuclei were counterstained with DAPI. For fluorescence microscopy, the images were acquired using an identical image acquisition time for all tissue sections. The images were acquired and analyzed using Leica TCS SP5 AOBS Resonant Scanning Multiphoton Confocal microscope. ImageJ software was used to quantitate the fluorescence analysis.

Real-Time RT-PCR

Total RNA from mouse epididymal fat, liver, choroid plexus, hippocampus, and cortex was extracted using RNeasy Lipid Tissue Mini Kit (QIAGEN). Total RNA was digested by DNase (Invitrogen). The cDNA synthesis and real-time RT-PCR were performed as described previously (BioRad) (Vandanmagsar et al., 2011). Quantitative real-time RT-PCR analyses were completed in duplicate on the ABI PRISM 7900 Sequence Detector TaqMan system with the SYBR Green PCR kit as instructed by the manufacturer (Applied Biosystems). GAPDH or 36B4 was used for normalization of mouse genes. The list of real-time PCR primers is shown in Table S1.

Western Blot Analysis

Mouse fat, spleen, and hippocampus were collected and immediately snap frozen in liquid nitrogen, then tissues were homogenized in liquid nitrogen using pestle and mortar to get powdered tissue. The immunoblot analysis was performed as described previously (Youm et al., 2012). The immune complexes were visualized by incubation with horseradish peroxidase-conjugated anti-rabbit or anti-rabbit secondary antibody (Amersham Biosciences). Immunoreactive bands were visualized by enhanced chemiluminescence (PerkinElmer Life Sciences).

Body Composition Analysis

Body composition parameters were measured using the Bruker minispec mq10 MRS (Bruker Optics, Germany). This analysis includes fat mass, lean tissue mass, free water, and today body water. Mice were placed in an acrylic tube with breathing holes and placed in the Minispec. The analyzer takes approximately 90 s and is based on Time Domain Nuclear Magnetic Resonance (TD-NMR) technology, which provides precise measurements in vivo. Data analysis is automated, and numerical results are then stored and analyzed further for evaluation.

MicroCT

Fixed femurs in 70% ethanol were scanned using the GE Explore μCT system at a voxel resolution of 20 μm from 720 views with a beam strength of 80 kvp and 450 μA. Integration time for each scan was 2,000 ms. Scans included bones from each condition and a phantom bone to standardize the grayscale values and maintain consistency between runs. Using the system's autothreshold (800) and isosurface analysis confirmation, bone mineral density (BMD) and content (BMC) and thickness were computed. Cortical bone measurements are determined with a 2 mm^3 region of interest (ROI) in the mid-diaphysis, with the exception of cortical BMD and BMC, which were made in a 0.1 mm^3 cube. Cortical thickness, moment of inertia, cortical area, marrow area, total area, inner perimeter, and outer perimeter, as well as all trabecular parameters, were computed using the GE Microview Software for visualization and analysis of volumetric image data.

Statistical Analyses

A two-tailed Student's t test was used to test for differences between genotypes or treatments: $^*p < 0.05$ and $p < 0.01$, $^{**}p < 0.005$ and $p < 0.001$. The results are expressed as the mean ± SEM. The differences between means and the effects of treatments were determined by one-way ANOVA using Tukey's test (Sigma Stat), which protects the significance ($p < 0.05$) of all pair combinations.

ACCESSION NUMBERS

Microarray experiments were designed to comply with MIAME guidelines (Brazma et al., 2001) and deposited in NCBI's Gene Expression Omnibus (Edgar et al., 2002). The data are accessible through GEO series accession number GSE43034 (http://www.ncbi.nlm.nih.gov/geo/query/acc.cgi?acc=GSE43034).

SUPPLEMENTAL INFORMATION

Supplemental Information includes seven figures and one table and can be found with this article online at http://dx.doi.org/10.1016/j.cmet.2013.09.010.

ACKNOWLEDGMENTS

We thank Dr. Vishva M. Dixit at Genentech, Inc. for providing anti-caspase-1 antibody, *Caspase-11*$^{-/-}$, *Nlrp3*$^{-/-}$, and *Asc*$^{-/-}$ mice. We also thank Pramod Mishra, Sarah McDaniels, and David Burk for excellent technical assistance. The research in the Dixit lab is supported in part by US National Institutes of Health (NIH) grants AG043608, AI105097, and DK090556 and the Pennington Foundation. H.M. was supported by NIH grant P20 RR02195 and J.M.S. by NIH grant HD055528.The present work utilized the facilities of the Genomics and CBB Core facilities supported by Pennington Center of Biomedical Research Excellence (NIH 8P20 GM103528) and Nutrition and Obesity Research Center (NIH P30 DK072476).

Received: March 14, 2013
Revised: July 7, 2013
Accepted: September 13, 2013
Published: October 1, 2013

REFERENCES

Brazma, A., Hingamp, P., Quackenbush, J., Sherlock, G., Spellman, P., Stoeckert, C., Aach, J., Ansorge, W., Ball, C.A., Causton, H.C., et al. (2001). Minimum information about a microarray experiment (MIAME)-toward standards for microarray data. Nat. Genet. *29*, 365–371.

Broderick, L., Gandhi, C., Mueller, J.L., Putnam, C.D., Shayan, K., Giclas, P.C., Peterson, K.S., Aceves, S.S., Sheets, R.M., Peterson, B.M., et al. (2013). Mutations of complement factor I and potential mechanisms of neuroinflammation in acute hemorrhagic leukoencephalitis. J. Clin. Immunol. *33*, 162–171.

Chalkiadaki, A., and Guarente, L. (2012). High-fat diet triggers inflammation-induced cleavage of SIRT1 in adipose tissue to promote metabolic dysfunction. Cell Metab. *16*, 180–188.

Claesson, M.J., Jeffery, I.B., Conde, S., Power, S.E., O'Connor, E.M., Cusack, S., Harris, H.M., Coakley, M., Lakshminarayanan, B., O'Sullivan, O., et al. (2012). Gut microbiota composition correlates with diet and health in the elderly. Nature *488*, 178–184.

Creely, S.J., McTernan, P.G., Kusminski, C.M., Fisher, M., Da Silva, N.F., Khanolkar, M., Evans, M., Harte, A.L., and Kumar, S. (2007). Lipopolysaccharide activates an innate immune system response in human adipose tissue in obesity and type 2 diabetes. Am. J. Physiol. Endocrinol. Metab. *292*, E740–E747.

Cutler, R.G., Kelly, J., Storie, K., Pedersen, W.A., Tammara, A., Hatanpaa, K., Troncoso, J.C., and Mattson, M.P. (2004). Involvement of oxidative stress-induced abnormalities in ceramide and cholesterol metabolism in brain aging and Alzheimer's disease. Proc. Natl. Acad. Sci. USA *101*, 2070–2075.

Czirr, E., and Wyss-Coray, T. (2012). The immunology of neurodegeneration. J. Clin. Invest. *122*, 1156–1163.

Dinarello, C.A. (2009). Immunological and inflammatory functions of the interleukin-1 family. Annu. Rev. Immunol. *27*, 519–550.

Duewell, P., Kono, H., Rayner, K.J., Sirois, C.M., Vladimer, G., Bauernfeind, F.G., Abela, G.S., Franchi, L., Nuñez, G., Schnurr, M., et al. (2010). NLRP3 inflammasomes are required for atherogenesis and activated by cholesterol crystals. Nature *464*, 1357–1361.

Edgar, R., Domrachev, M., and Lash, A.E. (2002). Gene Expression Omnibus: NCBI gene expression and hybridization array data repository. Nucleic Acids Res. *30*, 207–210.

Ferrucci, L., Corsi, A., Lauretani, F., Bandinelli, S., Bartali, B., Taub, D.D., Guralnik, J.M., and Longo, D.L. (2005). The origins of age-related proinflammatory state. Blood *105*, 2294–2299.

Franceschi, C., Bonafè, M., Valensin, S., Olivieri, F., De Luca, M., Ottaviani, E., and De Benedictis, G. (2000). Inflamm-aging. An evolutionary perspective on immunosenescence. Ann. N Y Acad. Sci. *908*, 244–254.

Franceschi, C., Capri, M., Monti, D., Giunta, S., Olivieri, F., Sevini, F., Panourgia, M.P., Invidia, L., Celani, L., Scurti, M., et al. (2007). Inflammaging and anti-inflammaging: a systemic perspective on aging and longevity emerged from studies in humans. Mech. Ageing Dev. *128*, 92–105.

Frisardi, V., Solfrizzi, V., Seripa, D., Capurso, C., Santamato, A., Sancarlo, D., Vendemiale, G., Pilotto, A., and Panza, F. (2010). Metabolic-cognitive syndrome: a cross-talk between metabolic syndrome and Alzheimer's disease. Ageing Res. Rev. *9*, 399–417.

Goronzy, J.J., and Weyand, C.M. (2005). T cell development and receptor diversity during aging. Curr. Opin. Immunol. *17*, 468–475.

Goto, M. (2008). Inflammaging (inflammation + aging): A driving force for human aging based on an evolutionarily antagonistic pleiotropy theory? Biosci Trends *2*, 218–230.

Green, D.R., Galluzzi, L., and Kroemer, G. (2011). Mitochondria and the autophagy-inflammation-cell death axis in organismal aging. Science *333*, 1109–1112.

Henao-Mejia, J., Elinav, E., Jin, C., Hao, L., Mehal, W.Z., Strowig, T., Thaiss, C.A., Kau, A.L., Eisenbarth, S.C., Jurczak, M.J., et al. (2012). Inflammasome-mediated dysbiosis regulates progression of NAFLD and obesity. Nature *482*, 179–185.

Heneka, M.T., Kummer, M.P., Stutz, A., Delekate, A., Schwartz, S., Vieira-Saecker, A., Griep, A., Axt, D., Remus, A., Tzeng, T.C., et al. (2013). NLRP3 is activated in Alzheimer's disease and contributes to pathology in APP/PS1 mice. Nature *493*, 674–678.

Ippagunta, S.K., Malireddi, R.K., Shaw, P.J., Neale, G.A., Walle, L.V., Green, D.R., Fukui, Y., Lamkanfi, M., and Kanneganti, T.D. (2011). The inflammasome adaptor ASC regulates the function of adaptive immune cells by controlling Dock2-mediated Rac activation and actin polymerization. Nat. Immunol. *12*, 1010–1016.

Kayagaki, N., Warming, S., Lamkanfi, M., Vande Walle, L., Louie, S., Dong, J., Newton, K., Qu, Y., Liu, J., Heldens, S., et al. (2011). Non-canonical inflammasome activation targets caspase-11. Nature *479*, 117–121.

Kayagaki, N., Wong, M.T., Stowe, I.B., Ramani, S.R., Gonzalez, L.C., Akashi-Takamura, S., Miyake, K., Zhang, J., Lee, W.P., Muszyński, A., et al. (2013). Noncanonical inflammasome activation by intracellular LPS independent of TLR4. Science *341*, 1246–1249.

Kotas, M.E., Jurczak, M.J., Annicelli, C., Gillum, M.P., Cline, G.W., Shulman, G.I., and Medzhitov, R. (2013). Role of caspase-1 in regulation of triglyceride metabolism. Proc. Natl. Acad. Sci. USA *110*, 4810–4815.

Lamming, D.W., Ye, L., Katajisto, P., Goncalves, M.D., Saitoh, M., Stevens, D.M., Davis, J.G., Salmon, A.B., Richardson, A., Ahima, R.S., et al. (2012). Rapamycin-induced insulin resistance is mediated by mTORC2 loss and uncoupled from longevity. Science *335*, 1638–1643.

Lumeng, C.N., Liu, J., Geletka, L., Delaney, C., Delproposto, J., Desai, A., Oatmen, K., Martinez-Santibanez, G., Julius, A., Garg, S., and Yung, R.L. (2011). Aging is associated with an increase in T cells and inflammatory macrophages in visceral adipose tissue. J. Immunol. *187*, 6208–6216.

Mariathasan, S., Weiss, D.S., Newton, K., McBride, J., O'Rourke, K., Roose-Girma, M., Lee, W.P., Weinrauch, Y., Monack, D.M., and Dixit, V.M. (2006). Cryopyrin activates the inflammasome in response to toxins and ATP. Nature *440*, 228–232.

Martinon, F., Pétrilli, V., Mayor, A., Tardivel, A., and Tschopp, J. (2006). Gout-associated uric acid crystals activate the NALP3 inflammasome. Nature *440*, 237–241.

Martinon, F., Mayor, A., and Tschopp, J. (2009). The inflammasomes: guardians of the body. Annu. Rev. Immunol. *27*, 229–265.

Masters, S.L., Dunne, A., Subramanian, S.L., Hull, R.L., Tannahill, G.M., Sharp, F.A., Becker, C., Franchi, L., Yoshihara, E., Chen, Z., et al. (2010). Activation of the NLRP3 inflammasome by islet amyloid polypeptide provides a mechanism for enhanced IL-1β in type 2 diabetes. Nat. Immunol. *11*, 897–904.

McGillicuddy, F.C., Harford, K.A., Reynolds, C.M., Oliver, E., Claessens, M., Mills, K.H., and Roche, H.M. (2011). Lack of interleukin-1 receptor I (IL-1RI) protects mice from high-fat diet-induced adipose tissue inflammation coincident with improved glucose homeostasis. Diabetes *60*, 1688–1698.

Miller, R.A., Kreider, J., Galecki, A., and Goldstein, S.A. (2011). Preservation of femoral bone thickness in middle age predicts survival in genetically heterogeneous mice. Aging Cell *10*, 383–391.

Morgan, T.E., Xie, Z., Goldsmith, S., Yoshida, T., Lanzrein, A.S., Stone, D., Rozovsky, I., Perry, G., Smith, M.A., and Finch, C.E. (1999). The mosaic of brain glial hyperactivity during normal ageing and its attenuation by food restriction. Neuroscience *89*, 687–699.

Naito, A.T., Sumida, T., Nomura, S., Liu, M.L., Higo, T., Nakagawa, A., Okada, K., Sakai, T., Hashimoto, A., Hara, Y., et al. (2012). Complement C1q activates canonical Wnt signaling and promotes aging-related phenotypes. Cell *149*, 1298–1313.

Neff, F., Flores-Dominguez, D., Ryan, D.P., Horsch, M., Schröder, S., Adler, T., Afonso, L.C., Aguilar-Pimentel, J.A., Becker, L., Garrett, L., et al. (2013). Rapamycin extends murine lifespan but has limited effects on aging. J. Clin. Invest. *123*, 3272–3291.

Netea, M.G., Joosten, L.A., Lewis, E., Jensen, D.R., Voshol, P.J., Kullberg, B.J., Tack, C.J., van Krieken, H., Kim, S.H., Stalenhoef, A.F., et al. (2006). Deficiency of interleukin-18 in mice leads to hyperphagia, obesity and insulin resistance. Nat. Med. *12*, 650–656.

Okin, D., and Medzhitov, R. (2012). Evolution of inflammatory diseases. Curr. Biol. *22*, R733–R740.

Pistell, P.J., Spangler, E.L., Kelly-Bell, B., Miller, M.G., de Cabo, R., and Ingram, D.K. (2012). Age-associated learning and memory deficits in two mouse versions of the Stone T-maze. Neurobiol. Aging *33*, 2431–2439.

Ransohoff, R.M., and Brown, M.A. (2012). Innate immunity in the central nervous system. J. Clin. Invest. *122*, 1164–1171.

Ruggiero, C., Cherubini, A., Ble, A., Bos, A.J., Maggio, M., Dixit, V.D., Lauretani, F., Bandinelli, S., Senin, U., and Ferrucci, L. (2006). Uric acid and inflammatory markers. Eur. Heart J. *27*, 1174–1181.

Shao, W., Yeretssian, G., Doiron, K., Hussain, S.N., and Saleh, M. (2007). The caspase-1 digestome identifies the glycolysis pathway as a target during infection and septic shock. J. Biol. Chem. *282*, 36321–36329.

Stienstra, R., van Diepen, J.A., Tack, C.J., Zaki, M.H., van de Veerdonk, F.L., Perera, D., Neale, G.A., Hooiveld, G.J., Hijmans, A., Vroegrijk, I., et al. (2011). Inflammasome is a central player in the induction of obesity and insulin resistance. Proc. Natl. Acad. Sci. USA *108*, 15324–15329.

Strowig, T., Henao-Mejia, J., Elinav, E., and Flavell, R. (2012). Inflammasomes in health and disease. Nature *481*, 278–286.

Vandanmagsar, B., Youm, Y.H., Ravussin, A., Galgani, J.E., Stadler, K., Mynatt, R.L., Ravussin, E., Stephens, J.M., and Dixit, V.D. (2011). The NLRP3 inflammasome instigates obesity-induced inflammation and insulin resistance. Nat. Med. *17*, 179–188.

Wang, S., Miura, M., Jung, Y.K., Zhu, H., Li, E., and Yuan, J. (1998). Murine caspase-11, an ICE-interacting protease, is essential for the activation of ICE. Cell *92*, 501–509.

Wen, H., Gris, D., Lei, Y., Jha, S., Zhang, L., Huang, M.T., Brickey, W.J., and Ting, J.P. (2011). Fatty acid-induced NLRP3-ASC inflammasome activation interferes with insulin signaling. Nat. Immunol. *12*, 408–415.

Youm, Y.H., Adijiang, A., Vandanmagsar, B., Burk, D., Ravussin, A., and Dixit, V.D. (2011). Elimination of the NLRP3-ASC inflammasome protects against chronic obesity-induced pancreatic damage. Endocrinology *152*, 4039–4045.

Youm, Y.H., Kanneganti, T.D., Vandanmagsar, B., Zhu, X., Ravussin, A., Adijiang, A., Owen, J.S., Thomas, M.J., Francis, J., Parks, J.S., and Dixit, V.D. (2012). The Nlrp3 inflammasome promotes age-related thymic demise and immunosenescence. Cell Rep *1*, 56–68.